

## Annealing effects on magnetic properties of silicone-coated iron-based soft magnetic composites

Shen Wu<sup>a</sup>, Aizhi Sun<sup>a,\*</sup>, Fuqiang Zhai<sup>a</sup>, Jin Wang<sup>a</sup>, Qian Zhang<sup>a</sup>, Wenhuan Xu<sup>a</sup>, Philip Logan<sup>b</sup>, Alex A. Volinsky<sup>b</sup>

<sup>a</sup> School of Material Science and Engineering, University of Science and Technology Beijing, Beijing 100083, China

<sup>b</sup> Department of Mechanical Engineering, University of South Florida, Tampa, FL 33620, USA

### ARTICLE INFO

#### Article history:

Received 21 July 2011

Accepted 22 September 2011

Available online 1 October 2011

#### Keywords:

Silicone resin

Soft magnetic composites

Annealing treatment

Permeability

### ABSTRACT

This paper focuses on novel iron-based soft magnetic composites synthesis utilizing high thermal stability silicone resin to coat iron powder. The effect of an annealing treatment on the magnetic properties of synthesized magnets was investigated. The coated silicone insulating layer was characterized by scanning electron microscopy and energy dispersive X-ray spectroscopy. Silicone uniformly coated the powder surface, resulting in a reduction of the imaginary part of the permeability, thereby increasing the electrical resistivity and the operating frequency of the synthesized magnets. The annealing treatment increased the initial permeability, the maximum permeability, and the magnetic induction, and decreased the coercivity. Annealing at 580 °C increased the maximum permeability by 72.5%. The result of annealing at 580 °C shows that the ferromagnetic resonance frequency increased from 2 kHz for conventional epoxy resin coated samples to 80 kHz for the silicone resin insulated composites.

© 2011 Elsevier B.V. All rights reserved.

### 1. Introduction

Soft magnetic composites (SMCs) are widely used in electromagnetic applications. They consist of ferromagnetic powder particles initially surrounded by an electrically insulating film. Powder metallurgy (PM) methods and annealing treatments are utilized to achieve desired properties in specific applications [1–4]. Insulated iron powder offers several advantages over traditional laminate steel in some applications. For example, the isotropic nature of the SMC, combined with new shaping methods, opens up possibilities for 3D design solutions [5–8]. The unique properties of the soft magnetic composite materials include magnetic and thermal isotropy, very low eddy current loss and a relatively low total core loss at low and medium frequencies, high magnetic permeability, high resistivity, a low anisotropy constant and low coercivity [9–13].

In order to achieve higher efficiency of soft magnetic materials in motor applications, they need to have higher density and electrical resistance. Processing pressure increase is a conventional method utilized to improve density and strength of the compressed SMCs. On the other hand, the high pressure also increases the dislocation density and the number of

imperfections, resulting in higher hysteresis losses. Therefore, an annealing treatment is employed to minimize the deleterious effects of cold working on the magnetic performance of the core material [14,15]. Organic and inorganic insulating coatings both increase the SMCs' resistivity [9,16,17]. Organic coatings are widely used in SMCs due to the rapid non-hazardous coating process and improved cured-film properties [18]. Compared with other PM processes, annealing is utilized less in conventional SMCs because the resistance temperature of phenolic or epoxy resin, when used as the insulating layer, is lower than 200 °C [19–21]. Therefore, choosing the high resistance insulation and the optimal annealing temperature has become a focus of modern SMCs development.

In this paper, a novel kind of SMC was prepared by utilizing silicone resin as the insulator, since its maximum thermal stability temperature exceeds 600 °C. This study focuses on investigating the effects of different annealing temperatures on the DC magnetic properties and the AC permeability of the synthesized SMCs.

### 2. Experimental details

#### 2.1. Materials

The iron powder was supplied by Licheng Co., Ltd. with particle size <150 μm. The purity of Fe was above 98%

\* Corresponding author. Tel.: 86 10 823 76835; fax: 86 10 623 33375.

E-mail addresses: [wuchen65174250@163.com](mailto:wuchen65174250@163.com) (S. Wu), [sunaizhi@126.com](mailto:sunaizhi@126.com) (A. Sun).

containing  $\sim 0.02$  wt% C, 0.01 wt% Cu, 0.01 wt% Zn and some oxides. 3-aminopropyltriethoxy silane (APTS, A1100) was used for the iron powder surface modification in order to create a uniform organic surface layer. The silicone resin (DC-805) consists mainly of polysiloxane and utilizes xylene as the auxiliary solvent. The 3-aminopropyltriethoxy silane and the silicone resin were supplied by Union Carbide and Dow Corning companies, respectively. The epoxy resin and the hardener are both widely used and were supplied by Fluka such that a comparison could be made.

## 2.2. Composite fabrication

The preparation of the SMCs was divided into two steps: the coating process and the PM process. In the first step, the iron powders were surface treated in APTS, which was diluted by a 95 vol% alcohol solution. In the surface treatment process, the iron powder to APTS mass ratio was adjusted to 100:1. To remove the additional coupling agent from the surface, the powders were washed three times in ethanol and were then dried at 50 °C. The modified iron powders were coated by being mixed with 4 wt% silicone resin (the modified iron powders to silicone resin mass ratio was 100:4). The silicone resin was dissolved in the xylene solvent, with the silicone resin to xylene mass ratio being adjusted to 1:10, and the solution was then blended with the powders in a spiral mixer. Lastly, the coated powders were dried at 150 °C for 1 h in order to ensure that the xylene had completely evaporated and that the silicone resin had adequately adhered.

In the second step, the insulated silicone resin and epoxy resin powders were compressed into toroidal samples (40 mm outer diameter, 32 mm inner diameter and 4 mm height) at 500 MPa pressure. The prepared samples were then annealed at 200 °C, 300 °C, 500 °C, 580 °C and 650 °C for 1 h, in nitrogen. For the purposes of comparison, the green compacts (without annealing) and the uncoated powders were prepared and their magnetic properties were subsequently measured.

## 2.3. Characterization

The silicone insulating layer was characterized via scanning electron microscopy (SEM, ZEISS EVO 18, Germany) coupled with energy dispersive X-ray Spectroscopy (EDS). The coverage of particles with the silicone coating was observed in SEM. After polishing, the compositional distribution of the coated powders was characterized via elemental line scanning. Both the maximum permeability and the saturation magnetic induction of the synthesized samples were measured by a  $B$ - $H$  curve analyzer (MATS-210SD, China). The complex permeability of the toroidal samples was measured by an AC performance tester (NIM-3000, China, 400 Hz–500 kHz) at low flux densities. The electrical resistivity measurement was performed using the four points probe method according to the ASTM D4496-87 standard.

## 3. Results and discussion

### 3.1. Silicone resin differential thermal analysis

Fig. 1 shows the differential thermal analysis (DTA) curve of the silicone resin, as measured at a heating rate of 10 K/min in air. The small endothermic peak, which appears at 150 °C, was caused by the volatility of the xylene contained within the silicone resin. There is a steep exothermic peak at 600 °C due to the oxidation of the silicone resin in air. Therefore, the maximum processing temperature that the silicone resin could withstand in air is about 600 °C.

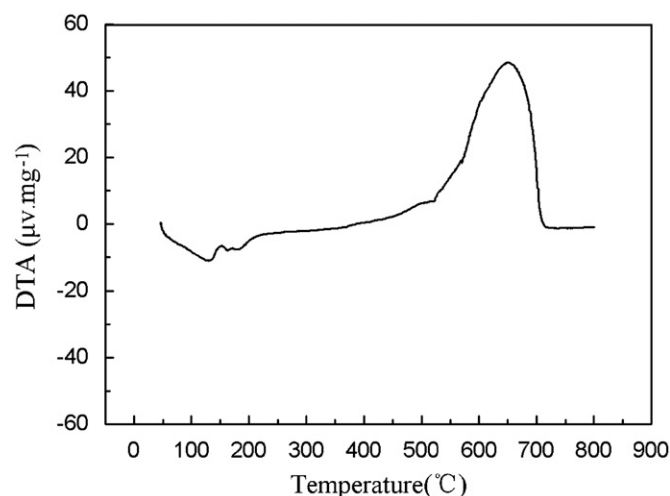


Fig. 1. DTA curve of the silicone resin in air.

### 3.2. Insulating layer characterization

Fig. 2(a) and Fig. 2 (b) show SEM micrographs of pure iron and the silicone coated iron powder particles, respectively. As can be seen, the coated iron powder exhibits fewer voids and metallic clusters. Fig. 2(c) shows the EDS analysis of the silicone coated iron powder. The surface layer of the iron powder consists of iron and silicon. Therefore, it is reasonable to assume that the silicone layer had formed around the iron powder particles, themselves. A comparison between the peak intensities of the silicon and the iron indicates that the silicon layer is thin.

Line scan mapping was utilized for further characterization after the samples were compacted. Fig. 3 depicts the maps of the iron and silicon distribution for a certain cross-section of the sample. Fig. 3(a) shows the selected line scanning area and direction. As shown in Fig. 3, the points A and B correspond to voids between the iron particles, whereas point C corresponds to a void in the iron particle itself. It is clear that the iron content reduced, while the silicon content increased significantly, along the boundaries of iron particles at points A and B. However, the silicon content did not change at point C, within the bulk of the iron particle itself. Based on these observations, it can be stated that each particle was coated by a uniform and thin silicone layer.

### 3.3. Magnetic properties

#### 3.3.1. Insulating layer effect on the magnetic properties

Fig. 4 shows the real part of the permeability of the uncoated samples, and the green silicone resin insulated samples, as a function of frequency. The change in the real part of the permeability of the silicone coated samples is almost negligible, which explains why the silicone coated samples have excellent frequency characteristics. At lower frequencies ( $< 20$  kHz), the real part of the permeability of the silicone coated samples is less than that of the uncoated samples. This can be explained by the silicone layer presence. Hence, a large fraction of non-magnetic material results in lower magnetic permeability. At higher frequencies ( $> 20$  kHz), the silicone powder, having a lower effective particle size, exhibits a higher magnetic permeability as a result of the eddy current reduction. The smaller eddy current means a larger skin depth, which leads to a higher operating frequency and, subsequently, lower losses at high frequencies [22].

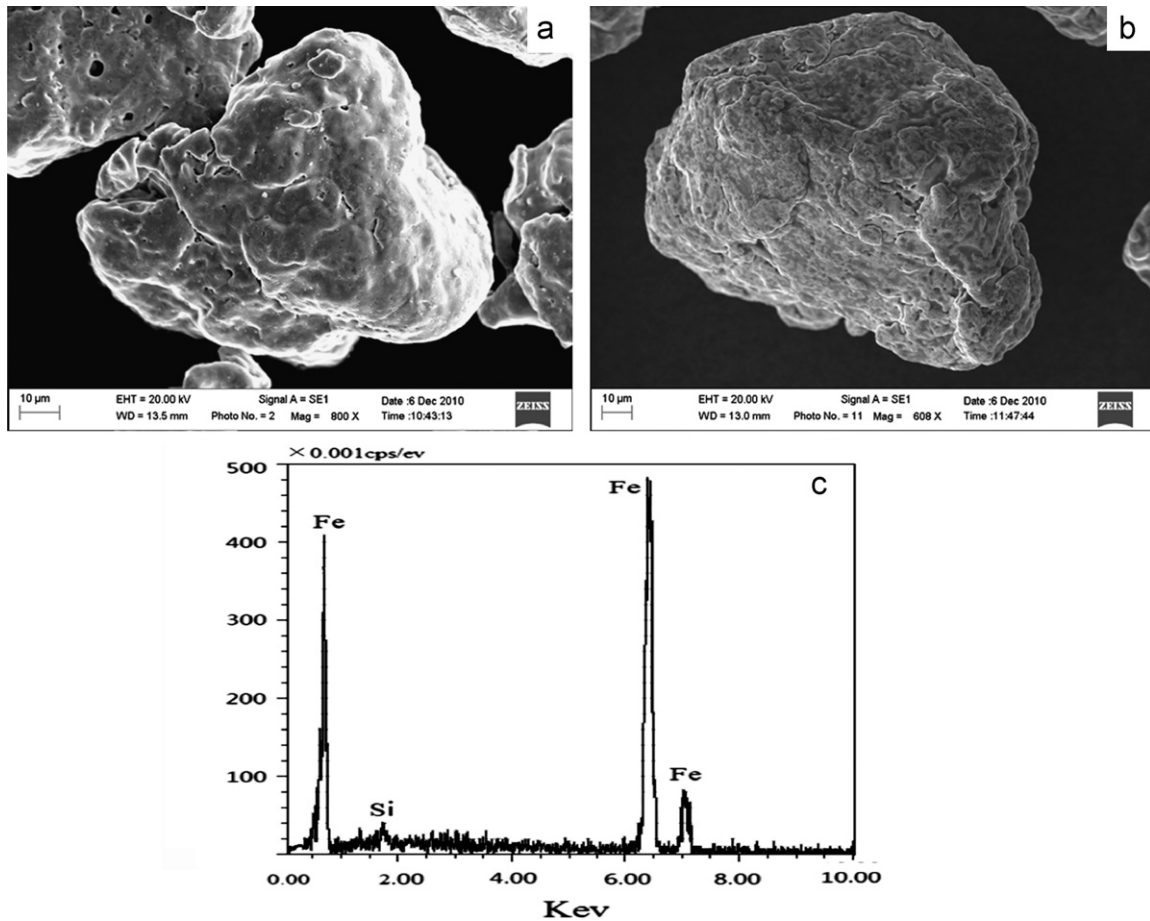


Fig. 2. SEM micrographs of (a) the pure iron powder; (b) the silicone resin coated iron powder; (c) EDS analysis of the silicone resin coated iron powder.

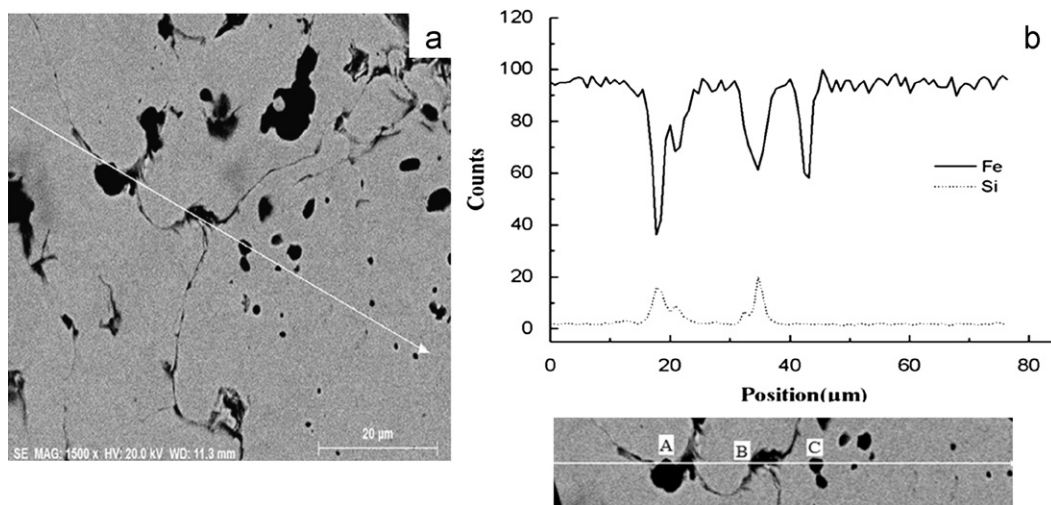
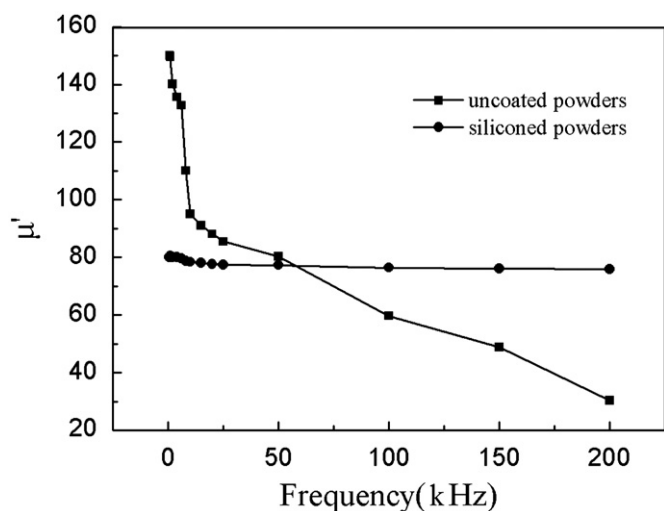


Fig. 3. (a) SEM image of the silicone-resin insulated compact showing EDS line scan and direction; (b) corresponding iron and silicon line profiles.

### 3.3.2. Annealing temperature effect on the magnetic properties

Although iron-resin composites are designed for AC magnetic applications, their DC characteristics are useful in better understanding their behavior when subjected to an alternating magnetic field, especially at low frequencies [23]. Table 1 depicts the effect of different annealing temperatures on the DC performance for a  $H_m = 5000 \text{ A m}^{-1}$  driving field. The annealing treatment increases the initial permeability, the maximum permeability, and the magnetic induction, and decreases the coercivity. The

heat treatment reduces distortions within the particles, lowers the dislocation density, and thereby increases the magnetic permeability [24]. Samples annealed at  $580^\circ\text{C}$  exhibit better DC properties, having a maximum permeability 72.5% greater than that of the non-annealed samples. The differences in the maximum permeability and the magnetic induction within the samples themselves, including those annealed at  $580^\circ\text{C}$  and  $650^\circ\text{C}$ , are negligible. This can be explained by the degradation of the silicone insulation at  $650^\circ\text{C}$ .



**Fig. 4.** Real part of the permeability for uncoated and green silicone resin insulated compacts.

**Table 1**  
Effect of annealing treatment at different temperatures on the DC performance ( $H_m = 5000 \text{ A m}^{-1}$ ).

Sample	Density ( $\text{g cm}^{-3}$ )	Initial permeability	Maximum permeability	Magnetic induction (mT)	Coercivity ( $\text{A m}^{-1}$ )
With silicone 4% (without annealing)	6.04	66.3	159.2	775.2	517.6
With silicone 4% (300 °C)	6.07	87.1	210.3	894.7	490
With silicone 4% (500 °C)	6.08	114.2	247.5	910.1	426.2
With silicone 4% (580 °C)	6.08	117.2	274.6	928.8	411.7
With silicone 4% (650 °C)	6.15	122.5	273.3	925.3	400.1

Fig. 5 shows the effect of the annealing temperature on the real and imaginary parts of the permeability. As shown in Fig. 5(a), the permeability of the annealed silicone sample is higher than that of the green sample. The reason for this is that the compaction step always creates some plastic deformation in the powder particles and, consequently, increases the dislocation density within the particles. The dislocations act as pinning centers and thus impede the movement of the magnetic domain walls. The heat treatment provides the low-volume fraction of defects, reduces the distortion within the particles, and lowers the dislocation density, thereby increasing the magnetic permeability [25]. The real part of the permeability continuously decreases with frequency, having a faster rate of decline at higher temperatures. Fig. 5(b) illustrates that the annealing treatment increases the magnitude of the imaginary part of the permeability, especially at higher temperature. The imaginary part of the permeability gradually increases after annealing at 300 °C, 500 °C and 580 °C for different frequencies. The imaginary part of the permeability has a maximum for the samples annealed at 650 °C, which corresponds to the resonant frequency [26]. The sample annealed at 650 °C exhibits a much lower electrical resistivity and a lower real permeability at high frequencies, whereas its imaginary permeability is higher at all frequencies. It has thus been confirmed that the insulating layer is failing at this annealing temperature. From Fig. 5, it is clear that the sample annealed at 580 °C has a higher real permeability and an acceptable imaginary permeability, in comparison with other annealed samples. As a result, it can be concluded that 580 °C is

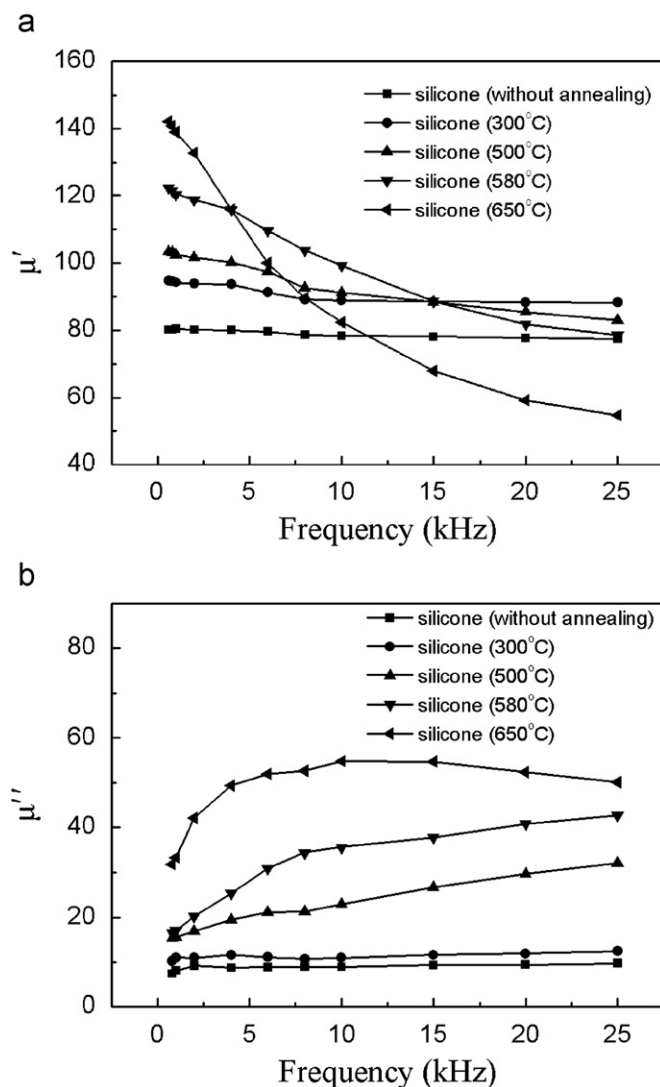


**Fig. 5.** Effect of annealing treatment at different temperatures on the permeability: (a) the real part and (b) the imaginary part.

**Table 2**  
Effect of annealing treatment on the electrical resistivity of silicon resin and epoxy resin coated compacts.

Electrical resistivity ( $\mu\Omega \text{ m}$ ) silicone resin	Electrical resistivity ( $\mu\Omega \text{ m}$ ) epoxy resin	Annealing temperature (°C)
401.3	284.7	Without annealing
297.2	170.9	200
213.5	53.5	300
69.5	12.6	500
54.1	8.5	580
16.7	3.2	650

a relatively ideal annealing temperature for silicone-coated, iron-based soft magnetic composites.

Table 2 shows the effect of an annealing treatment on the electrical resistivity of the silicon resin and epoxy resin coated compacts. As a general trend, the electrical resistivity decreased with the annealing temperature. The resistivity of the composite material strongly depends on the amount of resin and on defects such as porosity, point defects, residual stress, distortions and dislocation density. Annealing can reduce these imperfections and

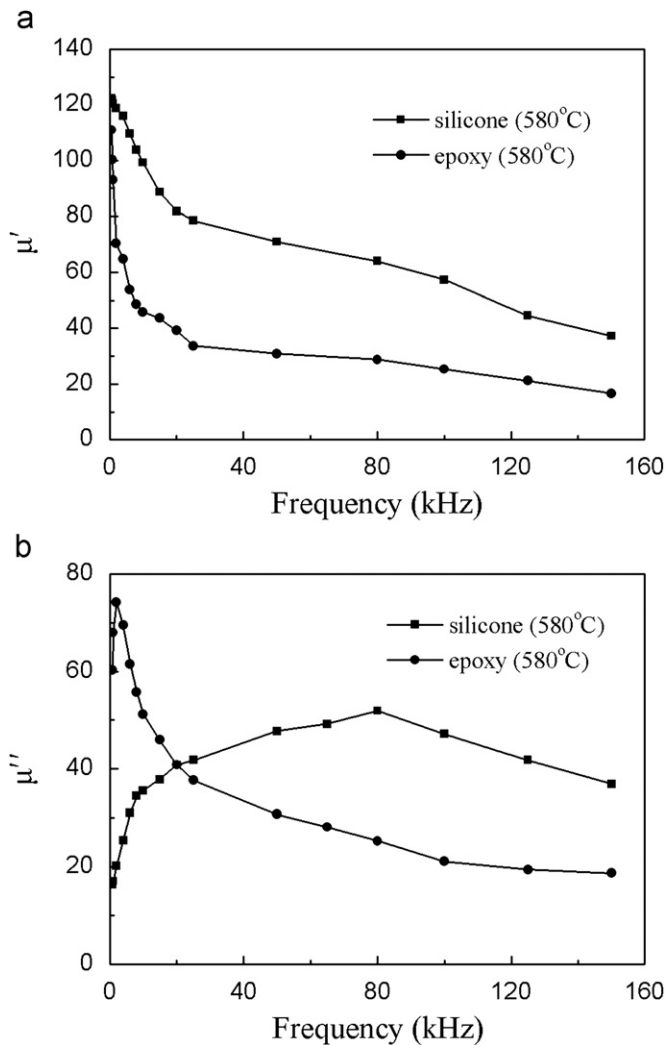


Fig. 6. Variation of the real and imaginary part of permeability with frequency for silicone resin and epoxy resin insulated compacts annealed at 580 °C.

release the residual stress. Therefore, annealed compacts have lower resistivity [27]. The resistivity of the samples with epoxy resin insulation sharply dropped at 300 °C, due to the epoxy resin's degradation, but the values of the resistivity for the silicone resin insulated samples are obviously greater than those of the epoxy resin compacts at each annealing temperature. Therefore, the silicone resin insulation has superior heat resistance when compared to the epoxy resin insulation.

Fig. 6(a) and (b) shows the real and imaginary permeability versus frequency for silicone resin and epoxy resin insulated compacts annealed at 580 °C. As shown in Fig. 6(a), the real part of the permeability of the samples coated with epoxy resin exhibits a lower value, which significantly decreased, even at the relatively low frequencies. This reduction results from degradation of the epoxy resin layer. This degradation severely decreases the electrical resistivity and increases the imaginary part of the permeability. Meanwhile, the ferromagnetic resonance frequency decreased from 80 kHz for the silicone resin powders to below 2 kHz for the epoxy resin insulated compacts, as shown in Fig. 6(b). The samples with silicone resin insulation possess higher electrical resistivity, a higher ferromagnetic resonance frequency, higher frequency stability and a lower imaginary permeability after annealing at 580 °C, as compared with the epoxy resin coated compacts.

#### 4. Conclusions

Iron-based soft magnetic composites with a silicone coating were investigated and the effect of an annealing treatment on the magnetic properties was studied. The following conclusions could be drawn:

1. SEM, EDX analysis, and element distribution maps showed that the particle surface layer contains a thin insulating layer of silicone with high particle surface coverage.
2. The silicone layer decreases the imaginary permeability, as well as increases the electrical resistivity and the operating frequency. For this reason, these samples have good magnetic characteristics in a wide range of frequencies.
3. Annealing increases initial permeability, maximum permeability, and magnetic induction, and decreases coercivity. For example, the maximum permeability for the sample annealed at 580 °C increases by about 72.5% when compared with the samples absent of annealing.
4. The SMCs with the silicone resin coating had higher electrical resistivity and lower imaginary permeability in a wide range of frequencies after annealing at 580 °C, as compared to the conventional epoxy resin coated samples.

#### References

- [1] E. Bayramli, O. Golgelioglu, H.B. Ertan, *Journal of Materials Processing Technology* 161 (2005) 83–88.
- [2] W.F. Miao, J. Ding, P.G. McCormick, R. Street, *Journal of Alloys and Compounds* 240 (1996) 200.
- [3] S. Gimenez, T. Lauwagie, G. Roebben, W. Heylen, O. Van der Biest, *Journal of Alloys and Compounds* 419 (2006) 299–305.
- [4] Y. Yoshizawa, S. Oguma, K. Yamauchi, *Journal of Applied Physics* 64 (1988) 6044–6047.
- [5] I.P. Gilbert, V. Moorthy, S.J. Bull, J.T. Evans, A.G. Jack, *Journal of Magnetism and Magnetic Materials* 242 (1) (2002) 232–234.
- [6] E. Enescu, P. Lungu, S. Marinescu, P. Dragoi, *Advanced Materials* 8 (2006) 745–748.
- [7] A.G. Jack, B.C. Mecrow, P.G. Dickinson, in: *Proceedings of IEEE International Electric Machines and Drives Conference*, Seattle, USA, 1999.
- [8] H. Amzaou I R, S. Gues sasma, O. Elkedim, *Journal of Alloys and Compounds* 462 (2008) 29–37.
- [9] C. Ishihara, T. Ito, K. Asaka, Hitachi Powdered Metals Technical Report, vol. 4, 2005, pp. 30–33.
- [10] K. Asaka, C. Ishihara, Hitachi Powdered Metals Technical Report, vol. 4, 2005, pp. 3–9.
- [11] H.R. Hemmati, H. Madaah Hosseini, A. Kianvash, *Journal of Magnetism and Magnetic Materials* 305 (2006) 147–151.
- [12] A. Ozolsa, M. Pagnolaa, D. Inaki Garciab, H. Sirkin, *Surface and Coatings Technology* 200 (2006) 6821–6825.
- [13] R. Bensalem, T. Ebib, S. Alleg, *Journal of Alloys and Compounds* 471 (2009) 24–27.
- [14] A.H. Morrish, *The Physical Principles of Magnetism*, John Wiley and Sons, Inc., 1965.
- [15] K. Suzuki, N. Kataoka, A. Inoue, A. Makino, T. Masumoto, *Journal of Applied Physics* 30 (1991) 1729.
- [16] O. Andersson, *High Velocity Compaction of Soft Magnetic Composites*, Hoganas, Sweden, 2002.
- [17] I. Chicinas, O. Geoffroy, O. Isnard, V. Pop, *Journal of Magnetism and Magnetic Materials* 310 (2007) 2474.
- [18] T. Madea, H. Toyoda, N. Igarashi, K. Hirose, K. Mimura, T. Nishikoa, A. Ikejaya, *SEI Technical Review* 60 (2005) 3–9.
- [19] H. Iwanabe, B. Lu, M.E. Mc Henry, D.E. Laughlin, *Journal of Applied Physics* 85 (1999) 4424.
- [20] A.H. Taghvaei, A. Ebrahimi, M. Ghaffari, K. Janghorban, *Journal of Magnetism and Magnetic Materials* 322 (2010) 808–813.
- [21] J.Y. Yang, J.S. Wu, T.J. Zhang, K. Chi, *Journal of Alloys and Compounds* 265 (1998) 269.
- [22] H. Shokrollahi, K. Janghorban, *Journal of Magnetism and Magnetic Materials* 313 (2007) 182–186.
- [23] H. Shokrollahi, K. Janghorban, *Journal of Materials Processing Technology* 189 (2007) 1–12.
- [24] Claude Gélinas, Donald Brydges, *Insulated Iron Powders for Automotive Applications [R]*, QMP Ltd., Canada, 2002 (pp. 2–5).
- [25] K. Nishimura, Y. Kohara, Y. Kitamoto, M. Abe, *Journal of Applied Physics* 87 (2000) 7127.
- [26] S. Chikazumi, *Physics of Magnetism*, Wiley, New York, 1964.
- [27] Y.G. Guo, J.G. Zhu, J.J. Zhong, *Journal of Magnetism and Magnetic Materials* 302 (2006) 14.